THE JOURNAL OF PHYSICAL CHEMISTRY C

Article

pubs.acs.org/JPCC

Efficient Energy Transfer and Enhanced Infrared Emission in Er-Doped ZnO-SiO_2 Composites

F. Xiao,[†,‡] R. Chen,[§] Y. Q. Shen,[∥] Z. L. Dong,[∥] H. H. Wang,[‡] Q. Y. Zhang,*[,†] and H. D. Sun*[,§]

[†]State Key Laboratory of Luminescent Materials and Devices and Institute of Optical Communication Materials and [‡]School of Chemistry and Chemical Engineering, South China University of Technology, Guangzhou 510641, PR China

[§]Division of Physics and Applied Physics, School of Physical and Mathematical Sciences, Nanyang Technological University, Singapore 637371, Singapore

[∥]Division of Materials Science, School of Materials Science and Engineering, Nanyang Technological University, Singapore 639798, Singapore

ABSTRACT: Intense near-infrared (NIR) emission around 1534 nm has been obtained from ZnO-SiO_2:Er^{3+} composites upon broadband ultraviolet light excitation. Remarkably, enhancement of the NIR emission as much as 20 times was achieved by optimal codoping with Li^+ ions. To elucidate the relevant mechanisms, comprehensive spectroscopic measurements have been performed on ZnO-SiO_2 composites with and without Er^{3+} ions doping. Photoluminescence spectroscopy and fluorescence decay dynamics clearly verify the efficient energy transfer from ZnO quantum dots (QDs) to Er^{3+} ions. Our results have not only demonstrated an efficient approach of color down-conversion but also indicated that ZnO-SiO_2:Er^{3+} composites could be a promising material for optical amplifier using broadband UV pumping.

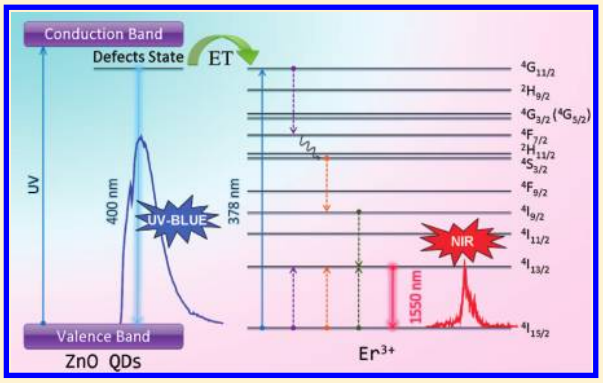

INTRODUCTION

Lanthanide-doped compounds have been widely utilized as high-performance materials in various devices such as optical amplifier and flat plane display based on their distinctive electronic, optical, and chemical properties arising from 4f electrons.[1−3] Among them, Er^{3+} ion is a well-known activator for solid-state laser in the infrared and visible region due to its characteristics of abundant energy level structure. The electronic transition from the first exited energy level $^4I_{13/2}$ to the ground state $^4I_{15/2}$ results in the emission around 1.54 μm located in the low-loss optical window for optical fiber communication. Meanwhile, the direct excitation of Er^{3+} is relatively inefficient due to the forbidden intra-4f transition. Moreover, the fluorescence from $^4I_{13/2}$ level can be easily quenched by phonon-assisted molecule collision.[4] To improve the near-infrared (NIR) luminescence efficiency of Er^{3+}, energy transfer from rare-earth (RE) ions to the Er^{3+} ions is studied, such as Ce^{3+}-Er^{3+} [4] and Eu^{2+}-Er^{3+}.[5] However, this kind of energy-transfer process can be realized only in limited hosts, whereas the energy-transfer process from a host material with broad absorption band to Er^{3+} ions is highly demanded but rarely reported.

Previously, it has been proved that the 1.54 μm NIR emission of Er^{3+} ions can be enhanced by utilizing wide band gap materials as the host owing to the resonant excitation of 4f electrons in Er^{3+} ions.[6] In the last two decades, ZnO has been recognized as a new-generation semiconductor material with excellent luminescence, magnetic, and optoelectronic properties, arising from its intrinsic features of wide band gap (3.37 eV) and a large exciton binding energy (60 meV).[7−9] With these characteristics, ZnO could be a potential host for harvesting ultraviolet energy. Therefore, RE^{3+}-doped ZnO has attracted strong interests due to the special application in visible and NIR region.[10−12] It has been shown that ZnO can provide a surrounding for the coexistence of Er and O, which may cause the formation of ErO_6 complex that can optically activate Er^{3+} ions.[13] Hence, ZnO may be considered as one of the promising hosts for Er^{3+} ions doping. However, the NIR emission efficiency of RE^{3+} ions in ZnO host under UV excitation is low due to the limited solubility of RE^{3+} ions. In this Article, we report on NIR emission of Er^{3+} caused by the energy transfer from ZnO QDs dispersed in SiO_2 matrix, and Li^+ ions were used as codopants to improve the emission intensity of Er^{3+}. On the basis of steady-state and time-domain spectroscopic data, the energy-transfer mechanism leading to the conversion of broad ultraviolet-blue (UV-blue) emission to NIR photons was discussed in detail. Furthermore, temperature-dependent NIR photoluminescence (PL) and the enhancement mechanism of NIR emission of Er^{3+} were investigated.

Received: April 27, 2012
Revised: May 29, 2012
Published: May 30, 2012

EXPERIMENTAL SECTION

$ZnO-SiO_2$ composites doped with 3 mol % Er^{3+} ions and different concentrations of Li^+ ions (Li^+ concentration = 0, 1, 3, 5, and 7 mol %) were prepared by a facile sol−gel method. The synthesis procedure is described as follows: 1 mmol zinc acetate-2-hydrate [$Zn(CH_3COOH)_2{\cdot}2H_2O$; Sigma-Aldrich, 99.999%] and LiOH (just for the samples doped with Li^+ ions) were dissolved in the mixture of moderate ethanolamine ($NH_2CH_2CH_2OH$) and absolute ethanol (analytical reagent) with constant stirring at 65 °C. Meanwhile, 4 mmol ethylorthosilicate (TEOS), ethanol, distilled water, and erbium nitric acid were mixed, followed by stirring for several hours at room temperature. Then, the above two solutions were mixed together and stirred for 4 h. The transparent gels were obtained after aging at room temperature for 1 week and subsequently dried at 60 °C for several days. Finally, the as-prepared bulk samples were calcinated at 600 °C for 2 h. This heat-treatment process stimulates the nucleation and growth of ZnO QDs.

High-resolution transmission electron microscopy (HRTEM) images were taken by using a JEOL JEM-2100F microscope (Cs = 0.5 mm, accelerating voltage = 200 kV). Photoluminescence (PL) and photoluminescence excitation (PLE) measurements of the undoped sample were characterized on a Shimadzu RF-5301PC spectrophotometer equipped with a 150 W Xenon lamp as the excitation source at room temperature. The NIR PL spectra were measured using the 325 nm line from a continuous-wave He−Cd laser as excitation source, the UV-blue emission was recorded by a photomultiplier, and the NIR emission was detected by a Peltier-cooled InGaAs photodiode using standard lock-in amplifier technique. The low-temperature PL measurements were performed by using a closed-cycle helium cryostat. The luminescence decay curve was obtained from a FLS920 fluorimeter (Edinburgh Instruments, Livingston, U.K.) with a hydrogen flash lamp (nF900, Edinburgh Instruments).

RESULTS AND DISCUSSION

Figure 1a shows the TEM image of $ZnO-SiO_2$ composite that contains ZnO QDs obtained by heat treatment at 600 °C for 2 h. It can be clearly seen that the ZnO QDs dispersed in amorphous SiO_2 matrix homogenously with the average size of 5 nm. The HRTEM image and the corresponding electron diffraction patterns are shown in Figure 1b,c, respectively. The well-distinguished lattice fringes in the HRTEM image corresponding to the (0 0 2) plane of ZnO with a *d* spacing of 0.26 nm indicate that the ZnO QDs are well-crystallized at the current annealing temperature. The electron diffraction pattern showing the spotty rings of (1 0 0), (0 0 2), (1 0 1), and (1 0 2) suggest the formation of wurzite ZnO.[14]

The ZnO QDs embedded in amorphous SiO_2 exhibit intense UV-blue emission under optical excitation. Figure 1d shows the normalized PLE and PL spectra of $ZnO-SiO_2$ composite at room temperature. The PLE spectrum monitored at 400 nm covers a broad band from 250 to 400 nm originating from carrier (or exciton) absorption by ZnO QDs. Upon optimal excitation wavelength of 338 nm, the PL spectrum exhibits a broad UV-blue emission band centered at 400 nm, which should originate from defects states related to oxygen vacancies near the band edge of ZnO.[15−17] These oxygen vacancies may be produced in the calcination process of $ZnO-SiO_2$ composite because the organic species such as TEOS and acetic acid would consume the oxygen. The silica layer around the ZnO QDs can slow down the diffusion of oxygen, which contributes to the recombination of photogenerated carriers trapped by interface states with deep trapped holes, leading to strong UV-blue emission. In addition, the amorphous SiO_2 matrix around ZnO QDs will reduce the density of surface dangling bonds, which can further minimize the nonradiative transition and visible deep level emission.[18] Therefore, the SiO_2 matrix plays an important passivation role in the UV-blue emission of ZnO QDs.

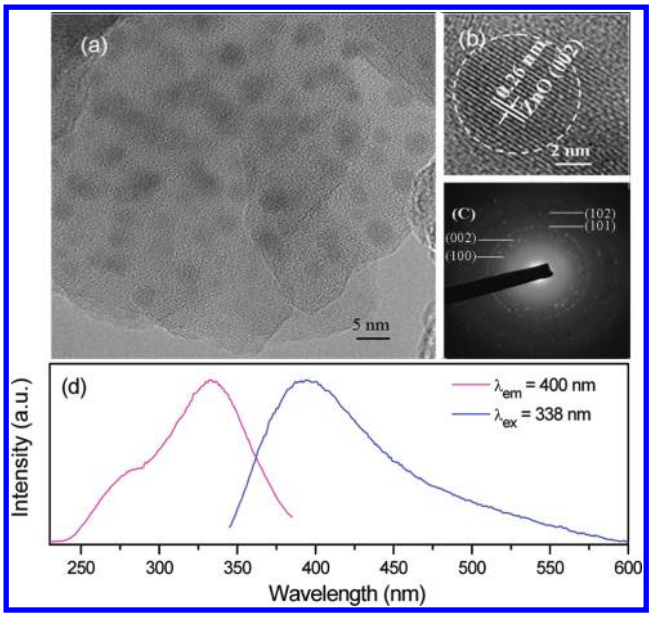

Figure 1. (a) TEM and (b) HRTEM image of $ZnO-SiO_2$ composite. (c) Electron diffraction pattern of the present region. (d) PLE and PL spectra of $ZnO-SiO_2$ composite.

Under UV excitation, the characteristic NIR emission of Er^{3+} is hardly observed in Er^{3+}-doped SiO_2 matrix, whereas two emission bands at visible and NIR region are simultaneously exhibited in Er^{3+}-doped $ZnO-SiO_2$ composite. As is shown in Figure 2, for $ZnO-SiO_2$:3% Er^{3+}, under the excitation of 338

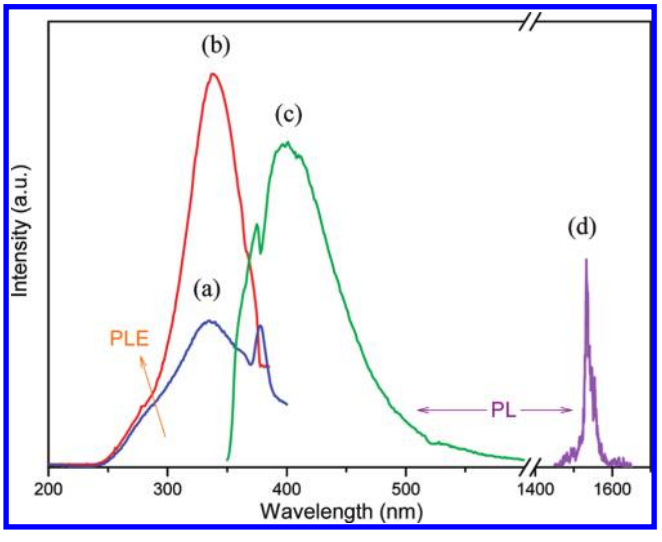

Figure 2. Fluorescence spectra of $ZnO-SiO_2$:3% Er^{3+} measured at room temperature: (a) PLE spectrum (λ_{em} = 1534 nm), (b) PLE spectrum (λ_{em} = 400 nm), (c) visible PL spectrum (λ_{ex} = 338 nm), and (d) NIR PL spectrum (λ_{ex} = 338 nm).

dx.doi.org/10.1021/jp304075g | J. Phys. Chem. C 2012, 116, 13458−13462

nm, the characteristic 1534 nm NIR emission due to the transition of $^4I_{13/2} \rightarrow {}^4I_{15/2}$ from Er^{3+} ions is exhibited, along with a strong visible broad emission band originated from ZnO-SiO_2 composite. Moreover, the visible spectrum component is different from that without Er^{3+} doping, characterized by a sharp emission band located at 378 nm due to the $^4I_{15/2}$-$^4G_{11/2}$ absorption of Er^{3+}.[19] The overlapping of the emission spectrum of ZnO-SiO_2 composite and intra-4f absorption of Er^{3+} may provide a channel to facilitate the energy transfer. To verify the energy transfer process from UV-blue emission of ZnO QDs to Er^{3+} ions, we measured the PLE spectra of ZnO-SiO_2:3% Er^{3+} composite. The excitation spectrum monitored at 1534 nm of Er^{3+} consists of a broad band centered at 338 nm and a sharp peak located at 380 nm originating from the $^4I_{15/2}$-$^4G_{11/2}$ transition of Er^{3+}, respectively. By comparison with the PLE spectrum of ZnO-SiO_2, the broad excitation band monitored at NIR emission of ZnO-SiO_2:3% Er^{3+} composite shows the same shape as that monitored at 400 nm, which provides convincing evidence that efficient energy transfer from ZnO QDs to Er^{3+} ions has been achieved.

Because of the spectral overlapping between donors and acceptors, the donor centers can relax either by direct energy transfer to acceptors (nonradiative energy transfer) or by first radiative recombination in the donor centers and then reabsorption by acceptors (radiative energy transfer). To distinguish the two processes, the decay lifetime of donors is analyzed. In principal, the luminescence lifetime would decrease in a nonradiative energy transfer process, whereas it would not be influenced by radiative reabsorption.[20] The PL decay curves of the ZnO-SiO_2 with and without Er^{3+}-doped composites with excitation at 338 nm and monitored at 400 nm were measured, as shown in Figure 3. It can be clearly seen that the UV-blue

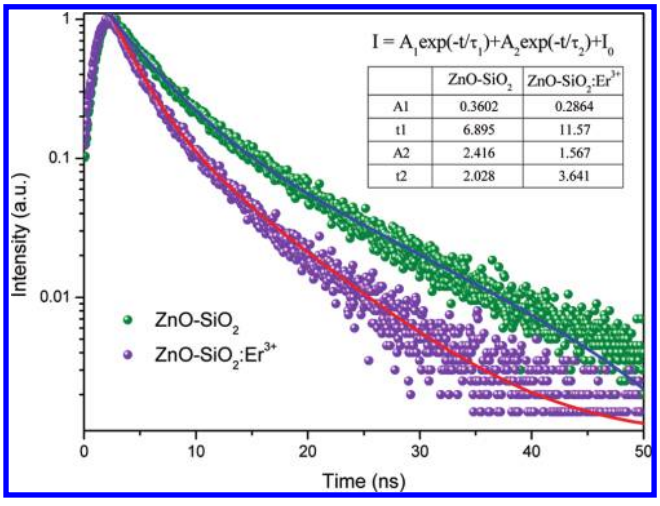

Figure 3. Luminescence decay curves of ZnO-SiO_2 and ZnO-SiO_2:3% Er^{3+} composite (λ_{ex} = 338 nm, λ_{em} = 400 nm).

emission from Er^{3+}-doped ZnO-SiO_2 decays faster than that of undoped composite, and both of the decay curves can be well-fitted by a biexponential equation with the expression of

$$I = A_1 \exp(-t/\tau_1) + A_2 \exp(-t/\tau_2) + I_0 \quad (1)$$

where I and I_0 are the luminescence intensities at time t and 0, A_1 and A_2 are fitting constants, and τ_1 and τ_2 are the fast and slow decay time (luminescent lifetime), respectively. The effective average lifetime τ^*_{eff} of near-UV emission can be estimated by the following equation[21]

$$\tau^*_{eff} = (A_1\tau_1^2 + A_2\tau_2^2)/(A_1\tau_1 + A_2\tau_2) \quad (2)$$

For the sample doped with Er^{3+} ions, the lifetime of UV-blue emission at 400 nm was calculated to be 3.7 ns, which is much shorter than that of 6.6 ns in the ZnO-SiO_2 composite without Er^{3+} doping. A plausible reason for the increased decay rate may be attributed to the Er^{3+} doping-induced nonradiative recombination centers, but the increased nonradiative recombination centers definitely do not contribute to the increase in infrared emission because the nonradiative recombination only dissipates the excited carriers. Because we have proven the effective energy transfer process from the PLE (λ_{em} = 1534 nm) and PL (λ_{ex} = 338 nm) spectra of the Er^{3+} doped ZnO-SiO_2 in Figure 2, it was proposed that the faster decay time of the UV-blue emission in Er^{3+}-doped composite should be dominated by the nonradiative energy transfer from ZnO QDs to Er^{3+} ions.

A simplified diagram of ZnO and Er^{3+} is depicted in Figure 4 to illustrate the possible mechanism of emission and energy

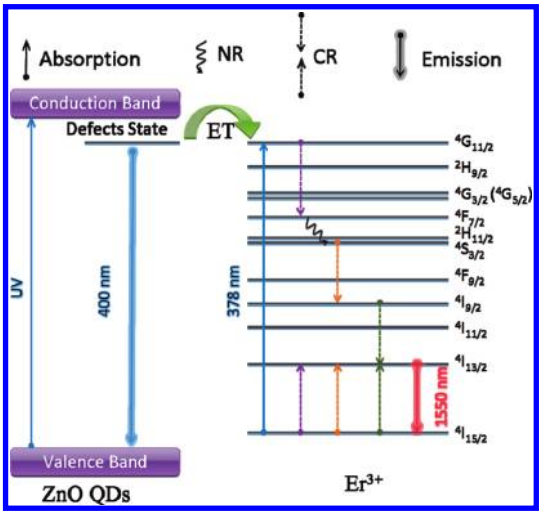

Figure 4. Schematic energy level diagram of the ZnO-SiO_2 composites and Er^{3+}, illustrating the possible mechanism of the UV-blue emission and energy transfer process for NIR emission. (ET and NR stand for energy transfer and nonradiative, respectively).

transfer process. Upon the UV excitation, most of the excited electrons in ZnO will radiatively relax to the ground state, resulting in the broad band emission centered at 400 nm. Meanwhile, part of the excited electrons were relaxed to Er^{3+} ions through the nonradiative energy transfer process, which finally results in the 1534 nm NIR emission. After the Er^{3+} ions located at ground state were excited and jumped to the $^4G_{11/2}$, the electrons then decayed to $^4F_{7/2}$ energy level, which would cause the Er^{3+} ions to jump from the $^4I_{15/2}$ to the $^4I_{13/2}$. By nonradiation transition from the $^4F_{7/2}$, the $^4S_{3/2}$ level was populated, followed by cross energy transfer of ($^4S_{3/2} \rightarrow {}^4I_{9/2}$, $^4I_{15/2} \rightarrow {}^4I_{13/2}$). Then, another cross energy transfer process of ($^4I_{9/2} \rightarrow {}^4I_{13/2}$, $^4I_{15/2} \rightarrow {}^4I_{13/2}$) consequently occurred.[22] Therefore, there should be three excitations to the $^4I_{13/2}$ level, which should greatly enhance the NIR luminescence efficiency of the Er^{3+}ions.

From the studies on NIR fluorescence of Er^{3+} ions, it is known that the electron−phonon interaction has great influence on the 1.54 μm emission.[23] To investigate the nonradiative decay process in Er^{3+}-doped ZnO-SiO_2 composite,

dx.doi.org/10.1021/jp304075g | J. Phys. Chem. C 2012, 116, 13458−13462

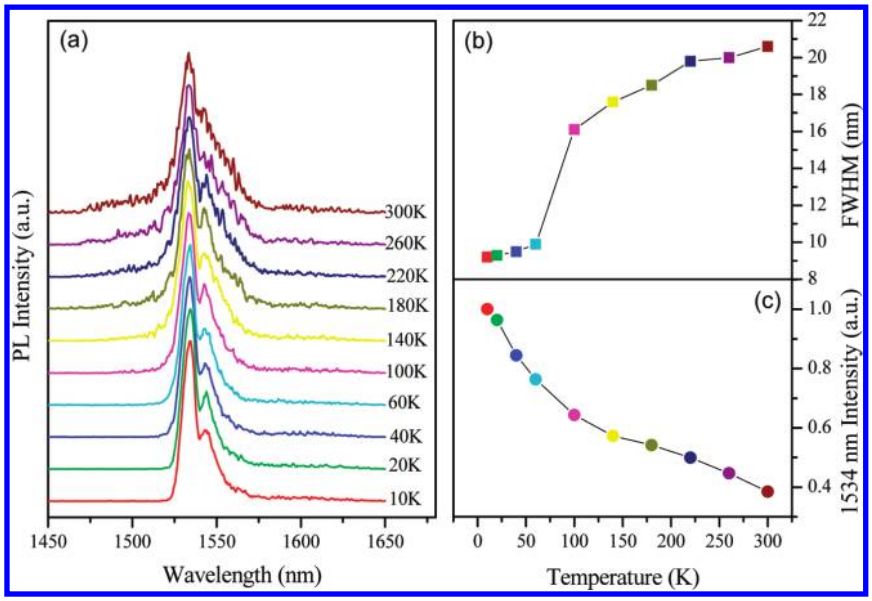

Figure 5. (a) Temperature-dependent PL spectra of ZnO-SiO_2:3% Er^{3+} composite. (b) Temperature dependence on the fwhm value of 1534 nm emission. (c) Temperature dependence on the 1534 nm emission intensity.

we measured the temperature-dependent PL spectra under the laser excitation at 325 nm. Figure 5a shows the normalized PL spectra in the temperature range from 10 to 300 K. Compared with the PL spectrum at room temperature, the sharper peaks originating from the $^4I_{13/2} \rightarrow {}^4I_{15/2}$ transition were clearly observed at 10 K. As the temperature gradually increased, the peak position located at 1534 nm remained unchanged, whereas the full width at half-maximum (fwhm) was increased from ~9 nm at 10 K to 20 nm at 300 K, as shown in Figure 5b. The broaden fwhm is due to the homogeneous broadening caused by nonradiative multiphonon relaxation. It is well known that the nonradiative transition probability by thermal activation will enhance with increasing temperature, then result in the quenching of NIR emission intensity. As depicted in Figure 5c, the emission intensity of 1534 nm was quenched by a factor of 60% as the temperature increased from 10 K to room temperature, which demonstrated the higher temperature limit than the Er^{3+}-doped III–V materials.[24]

In general, the energy transfer efficiency from semiconductor to RE ions is weak due to the limit solubility of RE in the host and weak interaction between carriers and RE ions.[25,26] For the actual application of RE-doped ZnO materials, improvement of their luminescence efficiency is essential. One of the most efficient ways is to decrease the aggregation of RE ions on the interface of grain by codoping with Li^+ ions. Furthermore, Li^+ ions can also lower the local symmetry around RE ions, which greatly enhances the emission intensity of RE ions.[27,28] Therefore, to enhance the NIR emission intensity of Er^{3+}, a series of 3 mol % Er^{3+} doped ZnO-SiO_2 composite with different concentrations of Li^+ ions was prepared. Figure 6 presents the room-temperature NIR spectra of Er^{3+}- and Li^+-codoped ZnO-SiO_2 composites under the 338 nm excitation. It is clearly shown that the emission intensity of 1534 nm increased dramatically with the increasing addition of Li^+ concentration without any shift of the strongest peak wavelength. It is well known that the intra-4f transition of an isolated Er^{3+} ion is forbidden. However, doping some impurities can bring down the symmetry of Er^{3+} ions' surrounding that causes a local distortion to make the

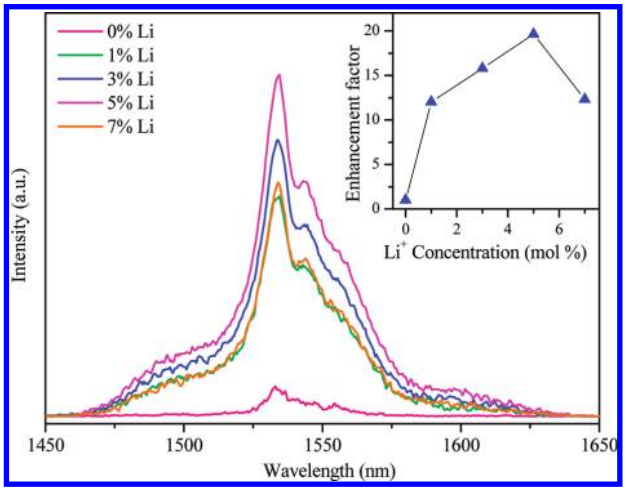

Figure 6. PL spectra of ZnO-SiO_2:3% Er^{3+} composite with different Li concentration at room temperature. The inset shows the enhancement factor of 1534 nm as a function of Li^+ ion concentrations.

forbidden intra-4f transition allowed. Here in the Er^{3+}- and Li^+- codoped ZnO-SiO_2 composite, the addition of small size Li^+ may occupy the interstitial sites ZnO-SiO_2 host or surround the ErO_6 cluster to maintain a local charge balance in some ways.[23] It has been suggested that the interstitial Li^+ will slightly modify the structure of ErO_6 cluster instead of destroy the structure, which leads to a lower symmetry of crystal field around Er^{3+} ions and then finally greatly enhances NIR luminescence of Er^{3+} ions. According to the previous research, the stark splitting is a sensitive indicator of the symmetry around Er^{3+} ions in the host matrix: the more stark levels, the lower symmetry of Er^{3+} ions.[20] Compared with the PL spectrum of Er^{3+}-doped ZnO-SiO_2 composite in Figure 6, a clear stark splitting was obviously observed with the Li addition, which provides an evidence of the lower symmetry of crystal field around Er^{3+} ions. Simultaneously, the incorporation of Li^+ ions will produce Li_{Zn}' defects, which can trap more holes and increase the recombination. This process would improve the energy transfer to Er^{3+} ions nearby. With Li^+ concentration

dx.doi.org/10.1021/jp304075g | J. Phys. Chem. C 2012, 116, 13458–13462

reaching up to 5%, the PL intensity at 1534 nm was significantly improved almost 20 times than that of the original ZnO-SiO_2:Er^{3+} composite without Li^+ doping, just as shown in the inset of Figure 6. After that, it decreased due to more defects form quench center caused by Li^+ ions doping. Previously, in Er^{3+}-doped optical amplifier, the pumping optical source was a laser with wavelength of 980 nm, where the pumping wavelength window is very narrow. The significance of our research is that such an optical amplifier can be pumped by a broadband optical source, so even an intense LED can be used as a pumping source.

CONCLUSIONS

In summary, NIR emission around 1534 nm of Er^{3+} ions has been realized in Er^{3+}-doped ZnO-SiO_2 composite upon broadband UV light excitation. Efficient energy transfer from ZnO QDs to Er^{3+} ions has been demonstrated by static spectroscopy and fluorescence decay curves. The Li^+ ion addition enhanced the integrate NIR emission intensity of Er^{3+} ions by ~20 times. The development of ZnO-SiO_2:Er^{3+} hybrid luminescent materials could open up a potential in realizing efficient optical amplifier based on broad-band optical source.

AUTHOR INFORMATION

Corresponding Author

*E-mail: qyzhang@scut.edu.cn, hdsun@ntu.edu.sg.

Notes

The authors declare no competing financial interest.

ACKNOWLEDGMENTS

This work was supported by NSFC (grant no. 51125005). Supports from the Singapore Ministry of Education through the Academic Research Fund (Tier 1) under project no. RG63/10 and from the Singapore National Research Foundation through the Competitive Research Programme (CRP) under project nos. NRF-CRP6-2010-02 and NRF-CRP5-2009-04 are gratefully acknowledged.

REFERENCES

(1) Macedo, A. G.; Ferreira, R. A. S.; Ananias, D.; Reis, M. S.; Amaral, V. S.; Carlos, L. D.; Rocha, J. *Adv. Funct. Mater.* **2010**, *20*, 624.
(2) Yang, J.; Li, C.; Cheng, Z.; Zhang, X.; Quan, Z.; Zhang, C.; Lin, J. *J. Phys. Chem. C* **2007**, *111*, 18148.
(3) Zhang, Q. Y.; Huang, X. Y. *Prog. Mater Sci.* **2010**, *55*, 353.
(4) Meng, J. X.; Cheah, K. W.; Shi, Z. P.; Li, J. Q. *Appl. Phys. Lett.* **2007**, *91*, 151107.
(5) Zhou, J. J.; Teng, Y.; Liu, X. F.; Ye, S.; Xu, X. Q.; Ma, Z. J.; Qiu, J. R. *Opt. Express* **2010**, *18*, 21663.
(6) Favennec, P. N.; L'Haridon, H.; Salvi, M.; Moutonnet, D.; Le Guillou, Y. *Electron. Lett.* **1989**, *25*, 718.
(7) Fan, X. F.; Sun, H. D.; Shen, Z. X.; Kuo Jer-Lai, Lu Y. M. *J. Phys.: Condensed Matters* **2008**, *20*, 235221.
(8) Zeng, H. B.; Cai, W. P.; Li, Y.; Hu, J. L.; Liu, P. S. *J. Phys. Chem. B* **2005**, *109*, 18260.
(9) Li, Y. Q.; Yang, Y.; Sun, C. Q.; Fu, S. Y. *J. Phys. Chem. C* **2008**, *112*, 17397.
(10) Mhlongo, G. H.; Ntwaeaborwa, O. M.; Swart, H. C.; Kroon, R. E.; Solarz, P.; Ryba- Romanowski, W.; Hillie, K. T. *J. Phys. Chem. C* **2011**, *115*, 17625.
(11) Yu, Y. L.; Wang, Y. S.; Chen, D. Q.; Huang, P.; Ma, E.; Bao, F. *Nanotechnology* **2008**, *19*, 055711.
(12) Chen, R.; Shen, Y. Q.; Xiao, F.; Liu, B.; Gurzadyan, G. G.; Dong, Z. L.; Sun, X. W.; Sun, H. D. *J. Phys. Chem. C* **2010**, *114*, 18081.
(13) Adler, D. L.; Jacobson, D. C.; Eaglesham, D. J.; Marcus, M. A.; Benton, J. L.; Poate, J. M.; Citrin, P. H. *Appl. Phys. Lett.* **1922**, *61*, 2181.
(14) Panigrahi, S.; Bera, A.; Basak, D. *ACS Appl. Mater. Interfaces* **2009**, *1*, 2408.
(15) Zeng, H. B.; Duan, G. T.; Li, Y.; Yang, S. K.; Xu, X. X.; Cai, W. P. *Adv. Funct. Mater.* **2010**, *20*, 561.
(16) Liu, K. W.; Chen, R.; Xing, G. Z.; Wu, T.; Sun, H. D. *Appl. Phys. Lett.* **2010**, *96*, 023111.
(17) Liu, K. W.; Tang, Y. D.; Cong, C. X.; Sum, T. C.; Huan, A. C. H.; Shen, Z. X.; Wang, L.; Jiang, F. Y.; Sun, X. W.; Sun, H. D. *Appl. Phys. Lett.* **2009**, *94*, 151102.
(18) Fu, Z. P.; Yang, B. F.; Li, L.; Dong, W. W.; Jia, C.; Wu, W. *J. Phys.: Condens. Matter* **2003**, *15*, 2867.
(19) Pan, Z. D.; Morgan, S. H.; Dyer, K.; Ueda, A.; Liu, H. M. *J. Appl. Phys.* **1996**, *79*, 8906.
(20) Miyakawa, T.; Dexter, D. L. *Phys. Rev. B: Solid State* **1970**, *1*, 2961.
(21) Xia, Z. G.; Wang, X. M.; Wang, Y. X.; Liao, L. B.; Jing, X. P. *Inorg. Chem.* **2011**, *50*, 10134.
(22) Chen, X. B.; Wu, J. G.; Xu, X. L.; Zhang, Y. Z.; Sawanobori, N.; Zhang, C. L.; Pan, Q. H.; Salamo, G. J. *Opt. Lett.* **2009**, *34*, 887.
(23) Schmidt, T.; Müller, G.; Spanhel, L. *Chem. Mater.* **1998**, *10*, 65.
(24) Neuhalfen, A. J.; Wessels, B. W. *Appl. Phys. Lett.* **1991**, *59*, 2317.
(25) Cheng, B. C.; Yu, X. M.; Liu, H. J.; Fang, M.; Zhang, L. D. *J. Appl. Phys.* **2009**, *105*, 014311.
(26) Gu, F.; Wang, S. F.; Lü, M. K.; Zhou, G. J.; Xu, D.; Yuan, D. R. *Langmuir* **2004**, *20*, 3528.
(27) Gu, X. Q.; Zhu, L. P.; Ye, Z. Z.; He, H. P.; Zhang, Y. Z.; Zhao, B. H. *Thin Solid Films* **2009**, *517*, 5134.
(28) Bai, Y.; Yang, K.; Wang, Y.; Zhang, X.; Song, Y. *Opt. Commun.* **2008**, *281*, 2930.